iJRASET
International Journal For Research in Applied Science and Engineering Technology

INTERNATIONAL JOURNAL FOR RESEARCH

IN APPLIED SCIENCE & ENGINEERING TECHNOLOGY

Volume: 9 **Issue:** VI **Month of publication:** June 2021

DOI: https://doi.org/10.22214/ijraset.2021.36026

www.ijraset.com

Call: 08813907089 | E-mail ID: ijraset@gmail.com

International Journal for Research in Applied Science & Engineering Technology (IJRASET)
ISSN: 2321-9653; IC Value: 45.98; SJ Impact Factor: 7.429
Volume 9 Issue VI June 2021- Available at www.ijraset.com

Effect of Edge Fluorination on Electronic and Transport Properties of Aarmchair Boron Nitride Nanoribbons: A First-Principles Study

Dr. Hari Mohan Rai
Department of Physics, Govt. P.G. College Tikamgarh, Tikamgarh, M.P.-472001, India

Abstract: ***We have systematically investigated the effect of edge fluorination on structural stability, electronic and transport properties of armchair boron nitride nanoribbons (ABNNRs), using first-principles calculations within the frame work of local spin-density approximation (LSDA). ABNNRs with F-passivation on only edge B atoms, regardless of their width, are found to be half-metallic and energetically most stable. For these ribbons, completely spin polarized charge transport is predicted across the Fermi level as a result of giant spin splitting. Transmission spectrum analysis also confirms the separation of spin-up and spin-down electronic channels. It is revealed that F-passivation of only edge N atoms transforms nonmagnetic bare ribbons into magnetic semiconductors whereas fluorination of both the edges does not affect the electronic and magnetic state of bare ribbons significantly. Predicted Half-metallicity projects these ABNNRs as potential candidates for inorganic spintronic devices.***
Keywords: DFT, BN-nanoribbons, DOS, Transmission Spectrum, LSDA

I. INTRODUCTION

The quasi-one 1-D thin strips carved out of hexagonal boron nitride (h-BN) sheet [1–4], appropriately known as BN nanoribbons (BNNRs), are of considerable research interest as they exhibit excellent structural stability and distinct electronic properties owing to the quantum confinement effects [1]. Depending on the definite shape of edges BNNRs are of two types - armchair BNNRs (ABNNRs) and zigzag BNNRs (ZBNNRs). It is already reported that the band gap (E_g) for ABNNRs with H-passivation on both the edges, oscillates periodically with increasing width [5] whereas the band gap of ZBNNRs decreases monotonically when both the edges are passivated by H atoms. [6,7] The experimental realization of these ribbons is already in existence as hollow BNNRs using B–N–O–Fe as precursor has already been synthesized by Chen. et al. [8]. In addition, Similar to their organic counterparts- 'Graphene Nanoribbons (GNRs)', BNNRs can also be fabricated from a single h-BN layer via lithographic patterning [9]. It has been already proven that BNNRs exhibit very fascinating electronic and transport properties similar to that of GNRs, [10,11] which are very important from the application point of view. For example, modification in electronic state/band gap of ABNNRs observed via Cl adsorption [12] and PH_3-passivation of ribbon edges [13], can be useful in gas sensor technology for sensing Cl and PH_3 gas molecules. Moreover, It has been already shown through first principles calculations that spin-polarization/half-metallicity [14] (the key property for spintronics devices) may be realized also in BNNRs either by chemically functionalizing zigzag edges with different groups such as H [15], F [16] and Cl [12] or with the application of an external in-plane electric field [17]. In previous study on ZBNNRs [6], we predicted that one-edge (only B-edge) H-termination makes the ribbons 'semi-metallic' in nature unlike 'half metallic' as predicted by Zheng et al. [15], but for spin polarized transport both of these results are in agreement with each other. Furthermore, spin-polarization has also been revealed theoretically in ZBNNRs through structural modifications (e.g., by making stirrup, boat, twist-boat etc.) [18] and through percentage hydrogenation [19]. However, from this spin-polarization perspective, ABNNRs barely explored in comparison with zigzag counterparts. By keeping in view that ABNNRs can also be potential spintronics elements, this article presents an attempt - to search the possibility of half-metallicity in ABNNRs via edge fluorination and to study the stability, electronic and transport properties of these edge fluorinated ribbons using DFT calculations.

A. Computational Details

Present first-principles calculations were performed with Atomistix Tool Kit-Virtual NanoLab (ATK-VNL) [20,21]. Presently employed simulation package i.e. ATK-VNL, is based on density functional theory (DFT) coupled with non-equilibrium Green's function (NEGF) formalism. The exchange correlation energy was approximated by local spin density approximation (LSDA) as proposed by Perdew and Zunger [22].

The reason for selecting, LDA is that the generalized gradient approximation underestimates the surface–impurity interactions [23]. The ABNNRs were modeled with periodic boundary conditions along z-axis, whereas the other two dimensions were confined. The energy cutoff value of 100 Rydberg was selected for the expansion of plane waves (Figure 1). We implemented double ζ plus polarized basis set for all the calculations. The k-point sampling was set to 1×1×100. In order to avoid artificial inter-ribbon interactions, ribbons were separated using a cell padding vacuum region of 10 Å. All the atoms, in the considered geometries, are relaxed and the optimization of atomic positions and lattice parameters has been continued until the forces on each constituent atom educed upto 0.05 eV/Å. We represent the ribbon-width by a width parameter Na, defined as the number of B/N atoms present in only one column of hexagons along the ribbon width as depicted in Figure 1, therefore, ABNNR with n B/N atoms across the ribbon is named as n-ABNNR.

II. RESULTS AND DISCUSSION

In present study, ABNNRs with – (i) both F-passivated edges ($ABNNR_{FBN}$) and (ii) only one F-passivated edge were considered for calculations. Furthermore, the ABNNRs belonging to later category are divided into two subgroups i.e., $ABNNR_{FB}$ and $ABNNR_{FN}$ depending upon whether only B or only N edge atoms are passivated by F-atoms respectively. The electronic and magnetic properties of bare ABNNRs have also been investigated and said ribbons were found to be nonmagnetic semiconductors, supporting the prediction by Ding et. al. [24]. In order to take size effects into considerations, presently, ABNNRs having widths N_a = 6 to 10 were investigated. Since the findings are qualitatively similar for symmetric ribbons (Odd N_a), the figures only for ABNNRs with N_a = 9 configuration are presented. Figure 1 schematically represents geometry of ABNNR in all presently considered ribbon configurations with N_a = 9 as representative case of different ribbon widths. The corresponding convention of super cell, used for simulation, is depicted by solid rectangle for presently investigated ribbon structures.

A. Electronic And Transport Properties

The calculated total DOS for all three considered edge fluorinated ribbons (N_a=9 as a representative case) are depicted all together in Figure 2. It is evident that both edge F-passivation ($ABNR_{FBN}$) makes ABNNR structures insulating in nature as the corresponding states nearest to Fermi level (dotted blue curves/peaks) in conduction band (CB) and valence band (VB), are separated well by an energy gap of > 4 eV. The electronic transmission spectrum (ETS) [6,10] plotted as transmission coefficient (TC) versus energy (Figure 3), also confirms this insulating nature of $ABNNR_{FBN}$ structures as the value of TC is zero in the corresponding energy window ranging between -3.5 eV to 0.8 eV. Further, the band gap (E_g) for $ABNNR_{FBN}$ structures is also calculated as a function of ribbon width and the same is tabulated in Table 1. It is clear from Table 1 that the value of E_g oscillates with increasing ribbon width which is a characteristic signature of ABNNRs [5]. The DOS for 9-$ABNNR_{FB}$ and 9-$ABNNR_{FN}$ are presented by red symbols (star) and green line respectively as shown in Figure 2. A significant difference in the form of giant splitting of spin-up and spin-down states can be clearly seen in DOS profiles of both of these ribbon structures. The corresponding ETS, depicted in Figure 3, also support this breaking of spin degeneracy for 9-$ABNNR_{FB}$ and 9-$ABNNR_{FN}$ respectively. This splitting of spin state gives rise to a net magnetic moment in the structure and hence irrespective of ribbon width an average magnetic moment of about 2.03 μ_B (2.02 μ_B) has been predicted for $ABNNR_{FB}$ ($ABNNR_{FN}$) structures. It is worth mentioning that the later magnetic moment has a little practical significance as it has been observed in $ABNNR_{FN}$ structures which are found to be energetically less stable by 3.6 eV than that of the $ABNNR_{FB}$ structures (as discussed later in stability analysis). Moreover, all $ABNNR_{FN}$ structures are found to be semiconducting in nature as the states (spin-up only) present nearest to the Fermi level, in CB and VB (green peaks-Figure 2) are separated by energy comparable with the band gap of a semiconductor. The value of corresponding TC, across the Fermi level, for 9-$ABNNR_{FN}$ is found to be zero in an energy window ranging from -0.5 eV to 1.7 eV for spin-up and from -2.55 eV to 0.5 eV for spin-down electronic transmission-states [Figure 3] indicating complete absence of any conducting channel across the Fermi level within the said energy ranges. This gap of energy observed between the transmission-states of corresponding spin warrants semiconducting behavior of 9-$ABNNR_{FN}$. On the other side, $ABNNR_{FB}$ structures are found to be half-metallic in nature because they are metallic for spin-down channels (since the peak corresponding to spin-down states is crossing Fermi level) and simultaneously they exhibit insulating behavior due to the presence of a large energy gap (>4 eV) between the spin-up states across the Fermi level as shown in Figure 2. In support, a small spin-down transmission peak (TC = 3) is observed at the Fermi level in the ETS of 9-$ABNNR_{FB}$ [Figure 3] also showing the presence of conducting states for spin-down electrons. Conversely, an energy window of about 4.5 eV, ranging from -0.3 eV to 4.2 eV, shows unavailability of any conducting channels for spin-up electrons as the value of TC is found to be zero for this energy range.

This half-metallic behavior is qualitatively independent of ribbon width and is observed for all investigated $ABNNR_{FB}$ structures. We predict that the charge transport across the Fermi level through all considered $ABNNR_{FB}$ structures should be entirely dominated by the spin-down electrons.

In order to understand the origin of half-metallicity in $ABNNR_{FB}$ structures, we analyzed that how the F-passivation/Fluorination of edge atoms affects DOS/ETS. It is found that the DOS /transmission states, which are available at Fermi level for $ABNNR_{FB}$, shifts away from Fermi level due to the passivation of edge N atoms with F for both $ABNNR_{FN}$ and $ABNNR_{FBN}$ [Figure 2 and 3]. This suggests that electronic charge which is localized at un-passivated edge N atoms is mainly responsible for the presence of electronic states at/across the Femi level in $ABNNR_{FB}$. Projected DOS (PDOS) analysis reveals that the peaks present at/across the Fermi level for $ABNNR_{FB}$ are predominantly composed of 2*p* orbital of un-passivated edge N atoms. Moreover, individually for each element, the bare on site Coulomb repulsion [16,25] has also been estimated as a difference between the first order ionization potential and electron affinity [16,26]. The estimated values were 14.01 eV for F, 8.02 eV for B and 14.79 eV for N. This large difference (≥ 5.99 eV) between N/F and B atoms hinders the charge transfer through edge-B atoms/B-F bond; therefore, the electrons are localized only in 2*p* orbital of un-passivated edge N atoms. In addition, the distance between any two adjacent edge N atoms (~2.43 Å) is large enough to ensure that no edge reconstruction has taken place, and there is consequently only one dangling bond per edge-N atom is present. This mechanism for the origin of half-metallicity is consistent with PDOS analysis and previous reports [16,27] on BNNRs. Eventually, the half-metallicity/spin polarization observed in $ABNNR_{FB}$ structures is entirely attributed to the localization of unpaired electrons at un-passivated edge N atoms.

B. Stability Analysis

Finally, to examine, which of the observed results are likely to be possible to realize experimentally, the relative stability of considered ribbon configurations has been calculated in terms of binding energy (E_B)/F-atom by using the following relation;

$$E_B = \frac{1}{x}\left[E_{tot}^{Configuration} - E_{tot}^{Bare} - xE_{tot}^{F}\right]$$

where, $E_{tot}^{Configuration}$, E_{tot}^{Bare}, and E_{tot}^{F} are the total energies of F-passivated ABNNR, bare ABNNR and isolated F atom respectively; x is the number of F atoms present in the ribbon structures under investigation. The calculated values of E_B for all three considered ribbon structures are plotted as function of ribbon width in Figure 4. It is to be noted that lower E_B represents higher stability. The perusal of Figure 4 indicates that irrespective of width, $ABNNR_{FB}$ structures are energetically most stable with lowest E_B amongst all considered configurations. The effect of ribbon width on E_B is found to be negligible as compared with the room temperature thermal energy (26 meV). $ABNNR_{FN}$ structures are ~3.6 eV lees stable as compared to $ABNNR_{FB}$ and the minimum E_B difference of ~820 meV is observed for $ABNNR_{FB}$ and $ABNNR_{FBN}$ structures which is large enough for any room temperature functionality. Present stability analysis predicts that amongst all presently studied edge fluorinated ABNNRs, the possibility of experimental realization is highest for $ABNNR_{FB}$ structures. In addition, we have also calculated the energy for spin polarized (E_{LSDA}) and spin compensated states (E_{LDA}) for all presently studied $ABNNR_{FB}$ structures. The spin polarized state is found to be ~0.4 eV ($\Delta E=|E_{LSDA}-E_{LDA}|$) more stable with respect to the spin compensated state (E_{LDA}). This difference is large enough for any room temperature operation and comparable to the values (0.17 eV, 3.5 meV and 48 meV) reported previously for ZBNNRs [15,18,19]. This large difference of about 0.4 eV along with the lowest E_B secures the place for present $ABNNR_{FB}$ structures (half-metals) as potential candidates in the field of spintronics. Moreover, the coupling between electrons of inter-edge un-passivated N atoms may be either ferromagnetic or antiferromagnetic, as the observed corresponding energies are found to be very close to each other [18]. Ultimately, present study reveals that electronic and transport properties of ABNNRs critically depend on the type of edge fluorination.

III. CONCLUSIONS

In summary, the effect of edge fluorination on the electronic and transport properties of ABNNRs has been systematically investigated using ab-initio calculations. $ABNNR_{FB}$ structures, regardless of ribbon width, are found to be half-metallic and energetically most favorable among all studied configurations. Electronic Transmission Spectrum analysis revealed that passivation of only edge-B (N) atoms via F atom i.e. $ABNNR_{FB}$ ($ABNNR_{FN}$) transforms non-magnetic insulating/semiconducting ABNNRs into magnetic half-metals (semiconductor) with TC = 3 at Fermi level for spin down states. The only one edge (B or N) fluorination also causes giant splitting of spin electronic states which gives rise to a substantial net magnetic moment of about 2.03 μ_B (or 2.02 μ_B) for

$ABNNR_{FB}$ ($ABNNR_{FN}$) structures. On the other hand, both-edge F-passivation of bare ABNNRs does not alter their electronic or transport behavior significantly; therefore, $ABNNR_{FBN}$ structures are non-magnetic insulators with degenerate/symmetric spin states similar to bare ABNNRs. Present findings suggest that the observed results can play a vital role towards the realization of inorganic spintronics devices.

IV. ACKNOWLEDGEMENTS

QuantumWise is acknowledged for providing trial version of ATK.

REFERENCES

[1] Y. Lin, J.W. Connell, Nanoscale 4 (2012) 6908.
[2] W. Auwärter, H.U. Suter, H. Sachdev, T. Greber, Chem. Mater. 16 (2003) 343.
[3] D. Pacilé, J.C. Meyer, Ç.Ö. Girit, A. Zettl, Appl. Phys. Lett. 92 (2008) 133107.
[4] W.-Q. Han, L. Wu, Y. Zhu, K. Watanabe, T. Taniguchi, Appl. Phys. Lett. 93 (2008) 223103.
[5] X. Wu, M. Wu, X.C. Zeng, Front. Phys. China 4 (2009) 367.
[6] H.M. Rai, N.K. Jaiswal, P. Srivastava, R. Kurchania, J. Comput. Theor. Nanosci. 10 (2013) 368.
[7] Z. Zhang, W. Guo, B.I. Yakobson, Nanoscale 5 (2013) 6381.
[8] Z.-G. Chen, J. Zou, G. Liu, F. Li, Y. Wang, L. Wang, X.-L. Yuan, T. Sekiguchi, H.-M. Cheng, G.Q. Lu, ACS Nano 2 (2008) 2183.
[9] M.Y. Han, B. Özyilmaz, Y. Zhang, P. Kim, Phys. Rev. Lett. 98 (2007) 206805.
[10] N.K. Jaiswal, P. Srivastava, IEEE Trans. Nanotechnol. 12 (2013) 685.
[11] N.K. Jaiswal, P. Srivastava, Solid State Commun. 152 (2012) 1489.
[12] P. Srivastava, N.K. Jaiswal, G.K. Tripathi, Solid State Commun. 185 (2014) 41.
[13] P. Srivastava, N.K. Jaiswal, V. Sharma, Superlattices Microstruct. 73 (2014) 350.
[14] Y.-W. Son, M.L. Cohen, S.G. Louie, Nature 444 (2006) 347.
[15] F. Zheng, G. Zhou, Z. Liu, J. Wu, W. Duan, B.-L. Gu, S.B. Zhang, Phys. Rev. B 78 (2008) 205415.
[16] Wang, Y. Ding, J. Ni, Phys. Rev. B 81 (2010) 193407.
[17] V. Barone, J.E. Peralta, Nano Lett. 8 (2008) 2210.
[18] D.K. Samarakoon, X.-Q. Wang, Appl. Phys. Lett. 100 (2012) 103107.
[19] W. Chen, Y. Li, G. Yu, C.-Z. Li, S.B. Zhang, Z. Zhou, Z. Chen, J. Am. Chem. Soc. 132 (2010) 1699.
[20] M. Brandbyge, J.-L. Mozos, P. Ordejón, J. Taylor, K. Stokbro, Phys. Rev. B 65 (2002) 165401.
[21] M. Chattopadhyaya, M.M. Alam, S. Sen, S. Chakrabarti, Phys. Rev. Lett. 109 (2012) 257204.
[22] J.P. Perdew, A. Zunger, Phys. Rev. B 23 (1981) 5048.
[23] J. Zhao, A. Buldum, J. Han, J.P. Lu, Nanotechnology 13 (2002) 195.
[24] Y. Ding, Y. Wang, J. Ni, Appl. Phys. Lett. 94 (2009) 233107.
[25] S. Dutta, A.K. Manna, S.K. Pati, Phys. Rev. Lett. 102 (2009) 096601.
[26] The data of ionization energy and electron affinity is adopted from http://chemed.chem.purdue.edu/genchem/topicreview/bp/ch7/ie_ea.html
[27] F. Zheng, K. Sasaki, R. Saito, W. Duan, B.-L. Gu, J. Phys. Soc. Jpn. 78 (2009) 074713.

Figures Tables

Table 1. Calculated Energy Band gap - E_g (eV) for $ABNNR_{FBN}$ structures with different ribbon widths.

Ribbon width N_a	E_g for $ABNNR_{FBN}$ (eV)
6	4.370
7	4.257
8	4.296
9	4.378
10	4.270

Figures

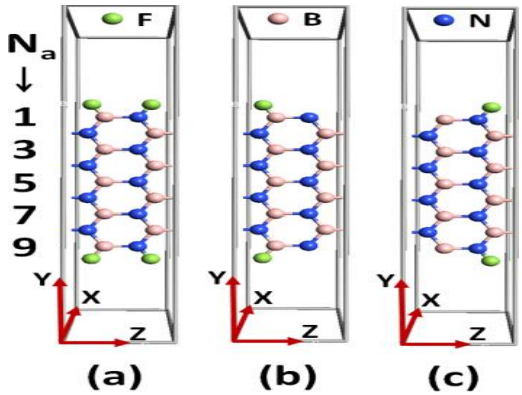

Figure 1

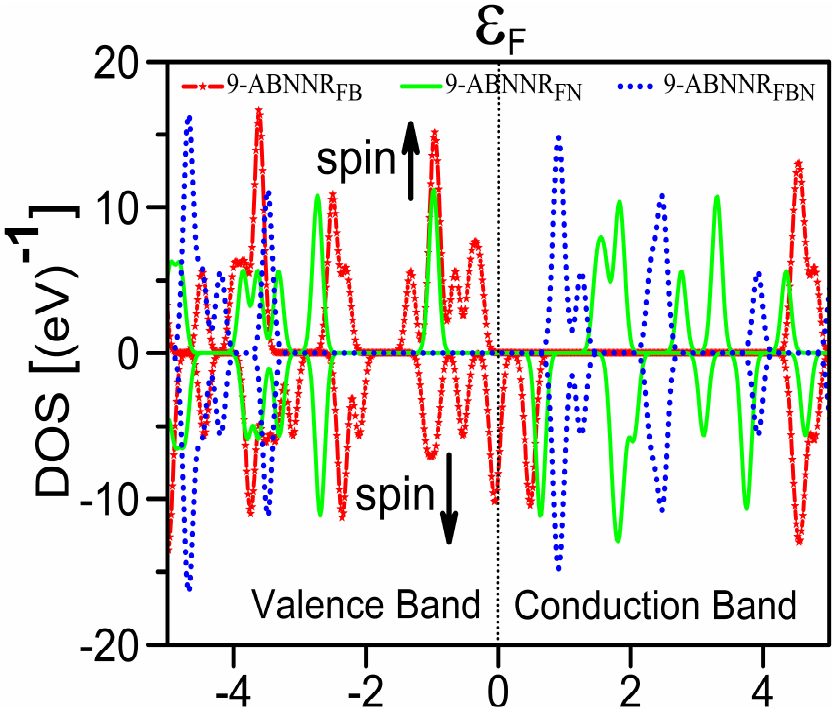

Figure 2

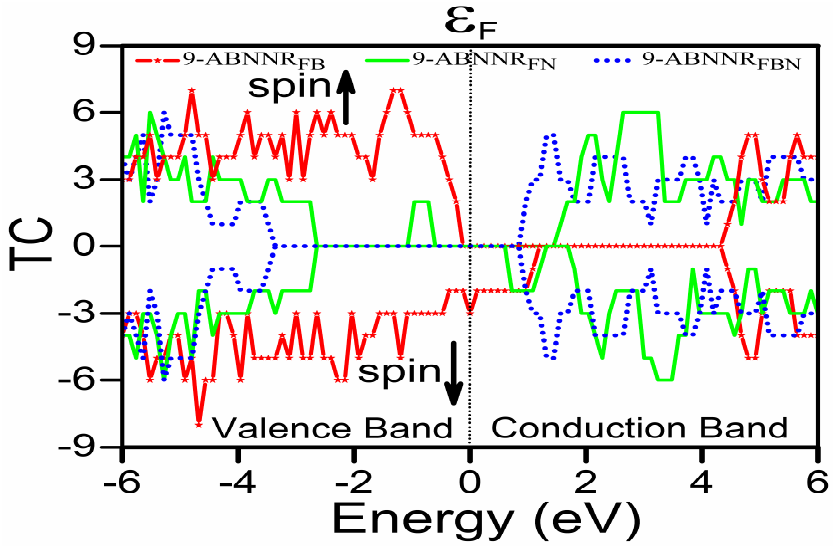

Figure 3

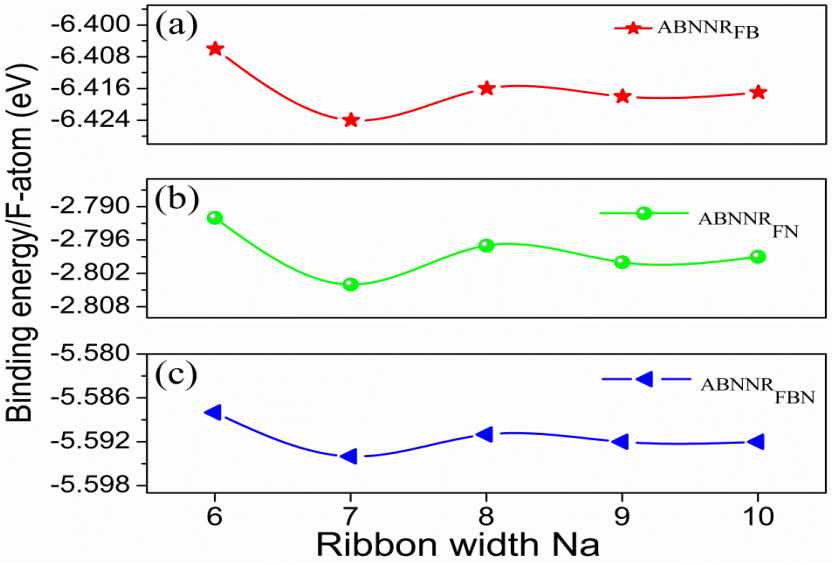

Figure 4

Figure captions

Figure 1: The schematic model for the convention of ribbon width and the supercell units (N_a=9) for (a) ABNNR$_{FBN}$, (b) ABNNR$_{FB}$ and (c) ABNNR$_{FN}$. The ABNNRs are modeled with periodic boundary conditions along *z*- axis whereas x and y directions are confined.

Figure 2: Calculated total DOS (N_a=9 as a representative case) for ABNNR$_{FB}$ –red, ABNNR$_{FN}$ –green and ABNNR$_{FBN}$ –blue. The positive and negative values of DOS are corresponding to spin-up and spin-down states respectively. The Fermi level is shown by a vertical dotted black line.

Figure 3: Calculated zero bias Transmission Coefficient (TC) for 9-ABNNR$_{FB}$-red, 9-ABNNR$_{FN}$-green and 9-ABNNR$_{FBN}$-blue. The positive and negative values of TC are corresponding to spin-up and spin-down states respectively. The Fermi level is shown by a vertical dotted black line.

Figure 4: Calculated Binding energy/F-atom (eV) as a function of ribbon width for (a) ABNNR$_{FB}$, (b) ABNNR$_{FN}$, and (C) ABNNR$_{FBN}$.

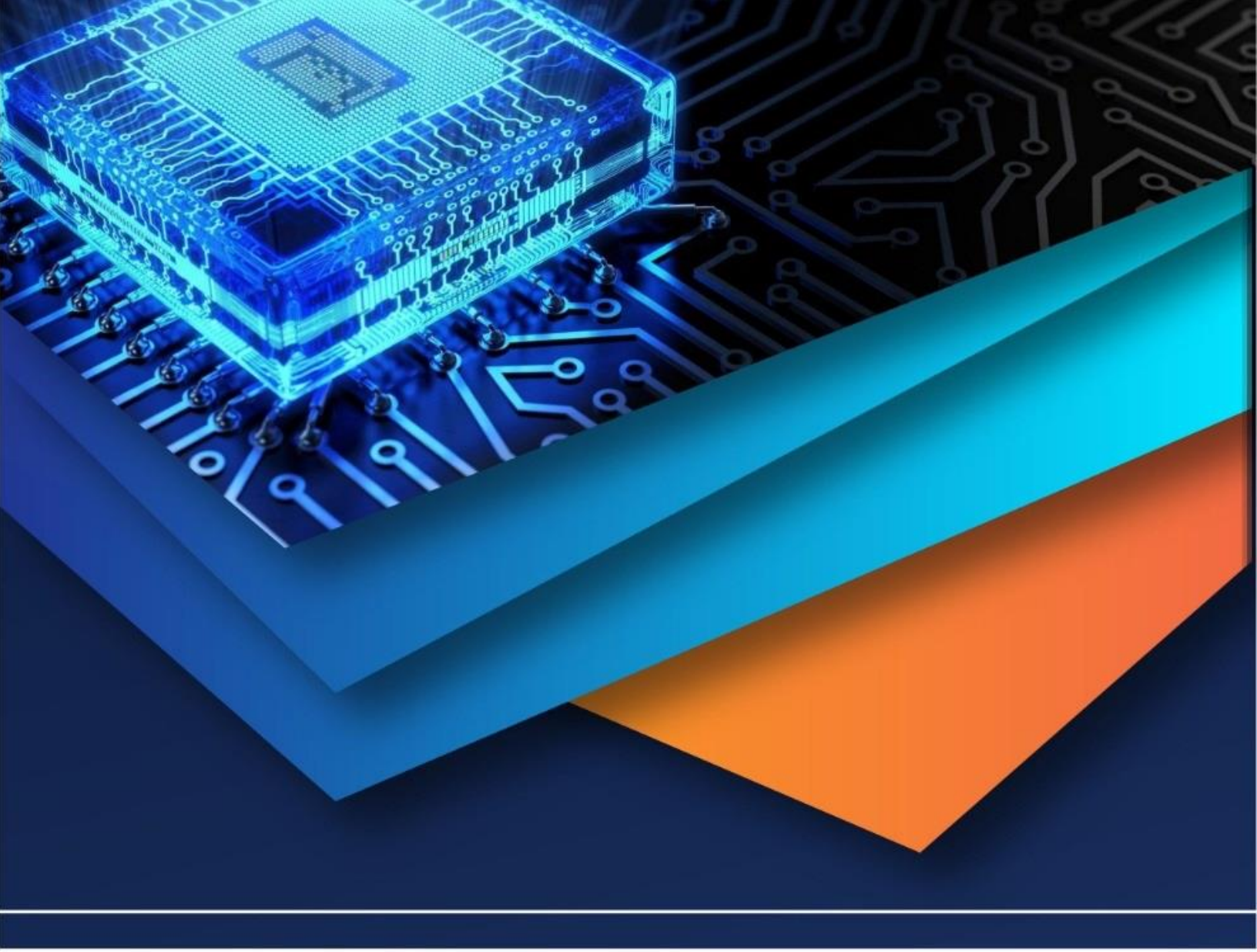

10.22214/IJRASET

45.98

IMPACT FACTOR: 7.129

IMPACT FACTOR: 7.429

INTERNATIONAL JOURNAL FOR RESEARCH

IN APPLIED SCIENCE & ENGINEERING TECHNOLOGY